JCB Article

Ca^{2+}-dependent redox modulation of SERCA 2b by ERp57

Yun Li and Patricia Camacho

Department of Physiology, University of Texas Health Science Center at San Antonio, San Antonio, TX 78229

We demonstrated previously that calreticulin (CRT) interacts with the lumenal COOH-terminal sequence of sarco endoplasmic reticulum (ER) calcium ATPase (SERCA) 2b to inhibit Ca^{2+} oscillations. Work from other laboratories demonstrated that CRT also interacts with the ER oxidoreductase, ER protein 57 (also known as ER-60, GRP58; ERp57) during folding of nascent glycoproteins. In this paper, we demonstrate that ERp57 overexpression reduces the frequency of Ca^{2+} oscillations enhanced by SERCA 2b. In contrast, overexpression of SERCA 2b mutants defective in cysteines located in intralumenal loop 4 (L4) increase Ca^{2+} oscillation frequency. In vitro, we demonstrate a Ca^{2+}-dependent and -specific interaction between ERp57 and L4. Interestingly, ERp57 does not affect the activity of SERCA 2a or SERCA 2b mutants lacking the CRT binding site. Overexpression of CRT domains that disrupt the interaction of CRT with ERp57 behave as dominant negatives in the Ca^{2+} oscillation assay. Our results suggest that ERp57 modulates the redox state of ER facing thiols in SERCA 2b in a Ca^{2+}-dependent manner, providing dynamic control of ER Ca^{2+} homeostasis.

Introduction

Changes in the cytosolic Ca^{2+} concentration control many essential cellular responses (Dolmetsch et al., 1997; Berridge et al., 1998; Li et al., 1998; Hajnoczky et al., 2003). To coordinate these functions Ca^{2+} signals are flexible, yet precisely regulated. At intermediate IP_3 concentrations (i.e., ~300 nM), cytosolic Ca^{2+} oscillates in *Xenopus* oocytes (Camacho and Lechleiter, 1993, 1995; John et al., 1998; Roderick et al., 2000; Falcke et al., 2003). Ca^{2+} oscillations are triggered by opening of the inositol 1,4,5-trisphosphate receptor (IP_3R) channel, whereas reuptake of the cation into the ER lumen is due to the activity of the sarco ER calcium ATPases (SERCAs). Consistent with this model, overexpression of SERCA pumps increases IP_3 induced Ca^{2+} oscillations (Camacho and Lechleiter, 1993). SERCA pumps play a critical role not only in clearing cytosolic Ca^{2+}, but also in maintaining ER Ca^{2+} concentrations ($[Ca^{2+}]_{ER}$). At rest, the free $[Ca^{2+}]_{ER}$ is ~300 μM, whereas cytosolic Ca^{2+} concentration is three to four orders of magnitude lower (~5–50 nM; Pozzan et al., 1994).

The lumen of the ER is a specialized protein-folding environment. It contains molecular chaperones such as calreticulin (CRT), calnexin (CLNX), and ER protein 57 (also known as ER-60, GRP58; ERp57; High et al., 2000; Ellgaard and Helenius, 2003; Kostova and Wolf, 2003; Schrag et al., 2003). Optimal $[Ca^{2+}]_{ER}$ is necessary for protein folding (Ashby and Tepikin, 2001). ER Ca^{2+} depletion inhibits protein folding and maturation (Hardman and Wetmore, 1996; Chen et al., 1997) and facilitates protein degradation (Ramsden et al., 2000). Ca^{2+} can also regulate the formation of chaperone complexes in the ER (Corbett et al., 1999).

ERp57 is a ubiquitous ER thiol-dependent oxidoreductase that promotes the formation of intra- or intermolecular disulfide bonds during glycoprotein folding (Marcus et al., 1996; High et al., 2000; Ellgaard and Helenius, 2003; Kostova and Wolf, 2003; Schrag et al., 2003). ERp57 has also been identified as a key component in the assembly of class I major histocompatibility complexes (Hughes and Cresswell, 1998; Lindquist et al., 1998; Morrice and Powis, 1998; Antoniou et al., 2002; Dick et al., 2002; Bouvier, 2003). Critical to our paper is the demonstration, firmly established in the literature, of a specific interaction between either CLNX or CRT with ERp57 (Oliver et al., 1997, 1999; Van der Wal et

Address correspondence to Patricia Camacho, Dept. of Physiology, MSC 7756, University of Texas Health Science Center at San Antonio, 7703 Floyd Curl Dr., San Antonio, TX 78229-3900. Tel.: (210) 567-6558. Fax: (210) 567–4410. email: camacho@uthscsa.edu

Key words: calreticulin; calcium ATPases; endoplasmic reticulum; calcium oscillations; glycoprotein folding

Abbreviations used in this paper: $[Ca^{2+}]_{ER}$, ER Ca^{2+} concentration; CLNX, calnexin; CRT, calreticulin; ERp57, ER protein 57 (also known as ER-60, GRP58); IP_3R, inositol 1,4,5-trisphosphate receptor; L4, loop 4; PDI, protein disulfide isomerase; SERCA, sarco ER calcium ATPase; $t_{1/2}$, decay time.

The Journal of Cell Biology, Volume 164, Number 1, January 5, 2004 35–46
http://www.jcb.org/cgi/doi/10.1083/jcb.200307010

The Journal of Cell Biology

al., 1998; Zapun et al., 1998; High et al., 2000; Frickel et al., 2002).

Our group discovered that CRT, as well as CLNX, inhibited Ca^{2+} oscillations using the *Xenopus* oocyte system (Camacho and Lechleiter, 1995; John et al., 1998; Roderick et al., 2000). The precise molecular mechanism responsible for this inhibitory effect is not completely known, however, CRT and CLNX may directly regulate SERCA 2b or they may recruit other enzymes such as ERp57 to cause the effect. Two conserved cysteines in the longest ER facing loop 4 (L4) of SERCA 2b are potential targets of ERp57. In this paper, we address the issues of whether ERp57 modulates Ca^{2+} oscillations through an interaction with L4 thiols; whether this interaction requires the enzymatic activity of ERp57; whether the interaction is specific and Ca^{2+} dependent; and whether CRT is required to recruit ERp57 to L4.

Results

Coexpression ERp57 with SERCA 2b reduces the frequency of Ca^{2+} oscillations

We used a confocal Ca^{2+} oscillation assay as a tool to investigate the modulation of the SERCA 2b pump activity. In this assay, increases in Ca^{2+} oscillation frequency (shorter period between oscillations and/or decay time [$t_{1/2}$] of individual waves) reflect increased Ca^{2+} ATPase activity and vice versa (Camacho and Lechleiter, 1993, 1995, 2000; John et al., 1998; Roderick et al., 2000; Falcke et al., 2003). To test whether ERp57 modulates SERCA 2b activity in *Xenopus* oocytes, we coexpressed SERCA 2b with ERp57. We found that coexpression reduced the frequency of Ca^{2+} oscillations compared with overexpression of SERCA 2b by itself. A histogram of period and $t_{1/2}$ shows that both were significantly prolonged suggesting that Ca^{2+} uptake into the ER is reduced (Fig. 1 A). Western blots demonstrated that expression levels of SERCA 2b were the same regardless of whether ERp57 was coexpressed with the pump (Fig. 1 B). These results are consistent with the hypothesis that ERp57 modulates ER thiol groups in SERCA 2b.

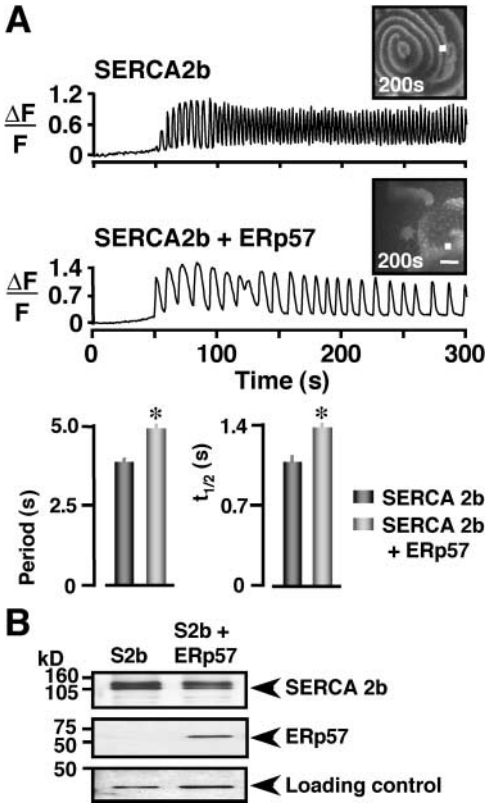

Figure 1. **ERp57 reduces the frequency of Ca^{2+} oscillations mediated by SERCA 2b.** (A) Confocal images of Ca^{2+} oscillations in *Xenopus* oocytes expressing SERCA 2b alone ($n = 22$) or coexpressing ERp57 with SERCA 2b ($n = 22$). Traces represent changes in fluorescence ($\Delta F/F$) as a function of time. Each plot represents two independent experiments with 11 oocytes per group. Individual Ca^{2+} wave images are presented at the indicated time. The white square in each and subsequent images represents a 5×5 pixel area used in determining $\Delta F/F$. Histogram plots of the period between oscillations and the decay time ($t_{1/2}$) are for individual oscillations at peak activity, defined as the highest frequency for a 100-s window of time. Asterisks indicate statistical significance ($P < 0.05$, *t* test). (B) Western blots of SERCA 2b and ERp57. One oocyte equivalent was loaded per lane and proteins were resolved through 10% SDS-PAGE. SERCA 2b migrates ~110 kD and ERp57 ~60 kD as expected. The loading control lane in each and subsequent gels represents an invariant *Xenopus* protein that migrates at ~42 kD. These gels represent three independent Western blots. Bar, 100 μm.

L4 cysteine–deficient mutants of SERCA 2b exhibit higher frequency of Ca^{2+} oscillations

To test whether the thiol groups in L4 are important in modulating Ca^{2+} oscillations enhanced by SERCA 2b, we imaged Ca^{2+} activity in oocytes overexpressing either the oxidizable form of SERCA 2b or two L4 cysteine–deficient mutants (SERCA 2b-C1SC2S and SERCA 2b-C1AC2A) that cannot form a disulfide bond and are a constitutively reduced form. Because these mutants did not express as efficiently as SERCA 2b in oocytes, we lowered expression levels of the pump to match expression levels of the mutants (Fig. 2 A). Under these conditions, we found that both mutants exhibited a higher frequency of Ca^{2+} oscillations and more rapid cytosolic Ca^{2+} uptake (i.e., shorter $t_{1/2}$) than SERCA 2b (Fig. 2 B). We also overexpressed a single missense mutation found in a Darier disease pedigree that involves a cysteine to glycine mutation in L4 (SERCA 2b-C875G; Ruiz-Perez et al., 1999; Sakuntabhai et al., 1999; Ahn et al., 2003). When overexpressed in the oocytes, this mutant also exhibited a higher frequency of Ca^{2+} oscillations than the wild-type SERCA 2b (unpublished data). Together, with the previous data, our results suggest that ERp57 promotes disulphide bond formation in L4, thereby reducing the activity of the Ca^{2+} pump. When the disulfide bridge in L4 is disrupted, the Ca^{2+} ATPase appears to exhibit higher pump activity.

Characterization of the catalytic activity of ERp57 and its mutants

Two conserved thioredoxin motifs in ERp57 are thought to be responsible for catalytic activity of the enzyme (Hirano et al., 1995). One motif is positioned near the NH_2-terminus (T1) and the other is near the COOH-terminus (T2). Two single mutants, ERp57-T1 and ERp57-T2, and a double

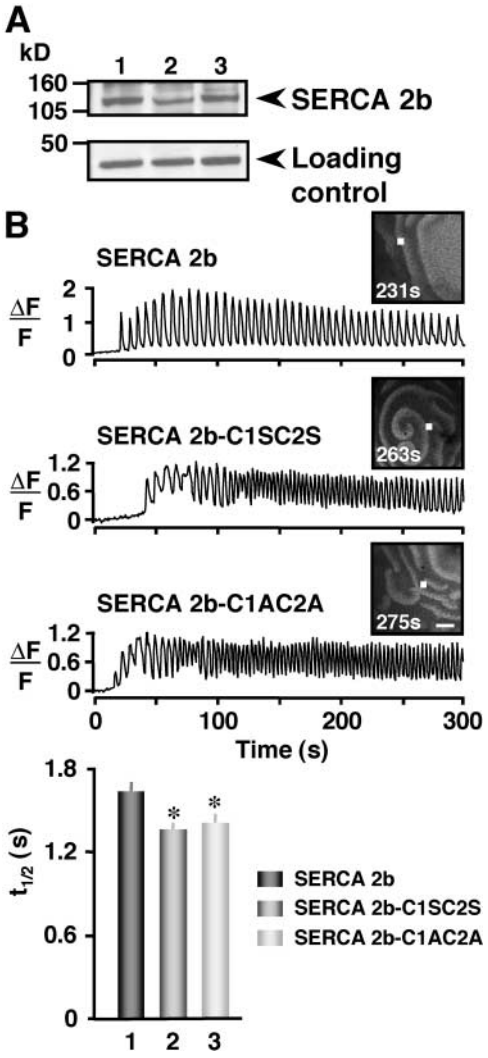

Figure 2. **L4 cysteine–deficient mutants of SERCA 2b exhibit higher frequencies of Ca^{2+} oscillations.** (A) Western blots of SERCA 2b and L4 mutants were loaded as follows: (lane 1) SERCA 2b, (lane 2) SERCA 2b-C1SC2S and (lane 3) SERCA 2b-C1AC2A. Two oocyte equivalents were loaded per lane and proteins were resolved through 12% SDS-PAGE. Gels represent four independent Western blots. (B) Confocal images of Ca^{2+} oscillations are shown in oocytes expressing SERCA 2b ($n = 34$) or the L4 cysteine–deficient mutants SERCA 2b-C1SC2AS ($n = 40$) and SERCA 2b-C1AC2A ($n = 38$). Traces represent two independent experiments with 15–20 oocytes per group. Histogram plots $t_{1/2}$ for (1) SERCA 2b, (2) SERCA 2b-C1SC2S, and (3) SERCA 2b-C1AC2A expressing oocytes. Asterisks indicate statistical significance ($P < 0.05$, *t* test) between SERCA 2b and each mutant group. Bar, 100 μm.

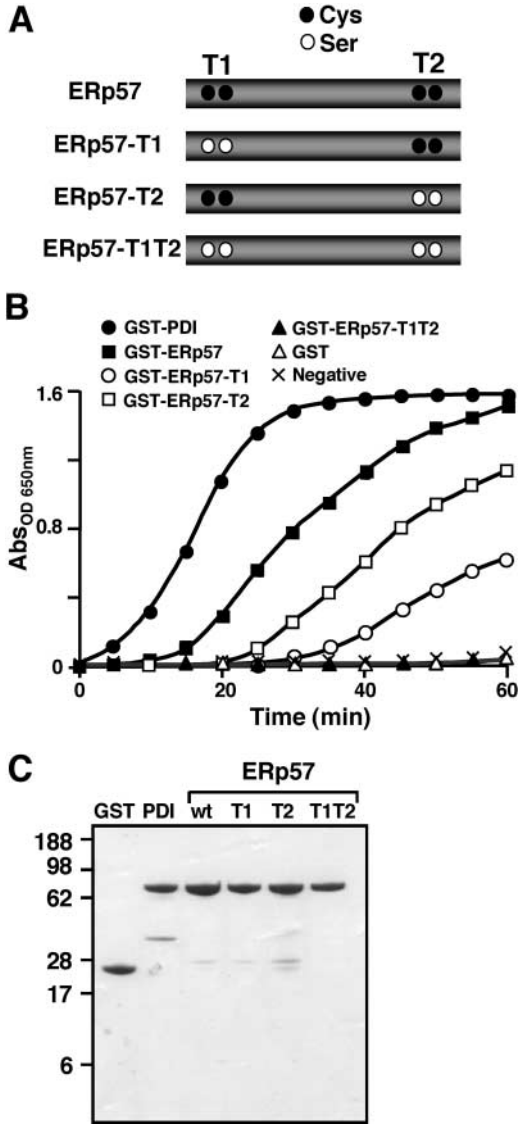

Figure 3. **Enzymatic activity of ERp57 and mutants measured in vitro.** (A) ERp57 mutants lacking thioredoxin motifs. Two conserved WCGHCK motifs of ERp57 are thought to be the active sites for thiol-dependent oxidoreductase activity. Cysteines in each motif are indicated in black circles. Mutagenesis of relevant cysteines into serines is indicated by white circles. (B) Thiol-dependent catalytic activity of GST-PDI (positive control) and GST-ERp57 or mutant GST-ERp57 fusion proteins measured in vitro by the insulin turbidity assay at 300 μM [Ca^{2+}]. GST alone and lack of enzyme input are used as negative controls in this assay. Triplicate $absorbance_{OD\ 650}$ values were taken in three independent experiments and plotted as a function of time. Input amount of GST fusion proteins was 0.8 μM except for GST (22.04 μM). (C) Coomassie blue staining of GST and GST fusion proteins as labeled after one-step affinity purification. Proteins (5 μg each) were resolved through 12% SDS-PAGE.

mutant, ERp57-T1T2, were generated by mutagenesis of the relevant cysteines into serines in each motif (Fig. 3 A). To characterize the mutant ERp57 proteins, we generated GST fusion proteins and measured in vitro the catalytic activity using an insulin turbidity assay (Holmgren, 1979; Hirano et al., 1995). Protein disulfide isomerase (PDI), another ER resident oxidoreductase, was used as a positive control for this assay. We cloned the rat isoform and made purified GST-PDI. Both GST-PDI and GST-ERp57 exhibited strong enzymatic activity, although the latter exhibited slower kinetics. In comparison to ERp57, the ERp57-T2 mutant exhibited ~70% activity, whereas the ERp57-T1 mutant exhibited only ~30% activity. The double mutation ERp57-T1T2 completely abolished ERp57 enzymatic activity. There was no activity when GST alone or enzyme was absent in the assay (Fig. 3 B). Purified GST and GST fusion proteins are shown (Fig. 3 C). Together, these results suggest that the T1 motif plays a critical role in ERp57 enzymatic activity.

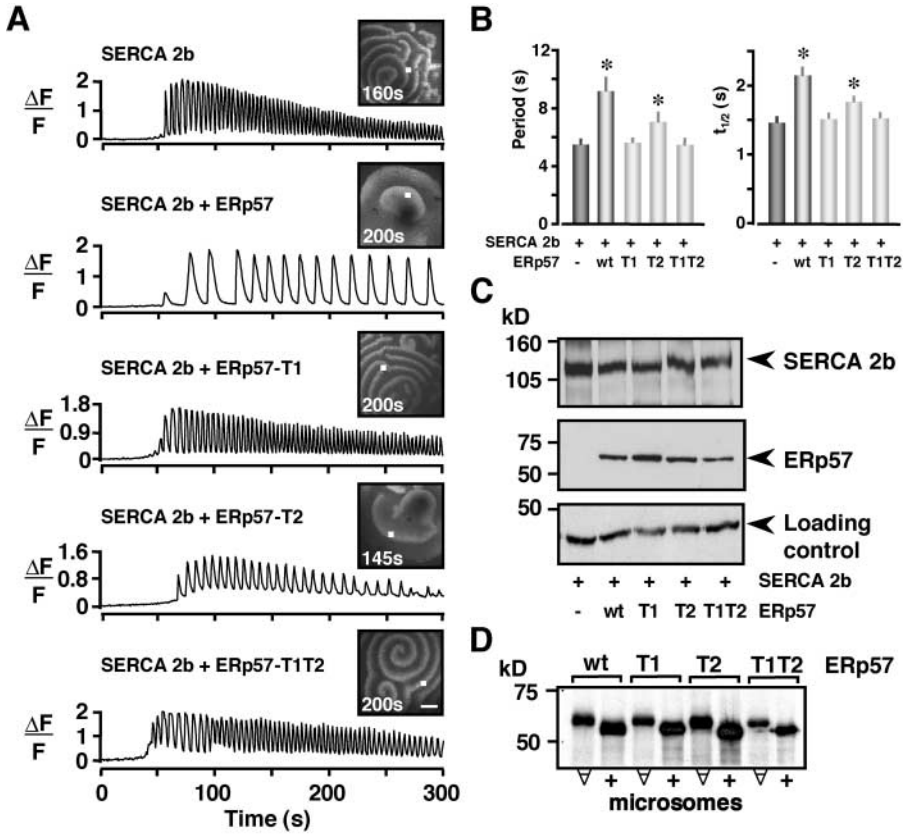

Figure 4. **Enzymatic activity of ERp57 plays a critical role in modulating SERCA 2b.** (A) Confocal images of Ca^{2+} oscillations shown in oocytes overexpressing proteins as labeled: SERCA 2b alone ($n = 23$); SERCA 2b + ERp57 ($n = 24$); SERCA 2b + ERp57-T1 ($n = 20$); SERCA 2b + ERp57-T2 ($n = 23$); and SERCA 2b + ERp57-T1T2 ($n = 32$). Traces represent two independent experiments with 11–15 oocytes per group. (B) Histograms of period and $t_{1/2}$ for the experiment in A. Asterisks indicate statistical significance ($P < 0.05$, *t* test) between SERCA 2b and SERCA 2b + ERp57 or SERCA 2b + ERp57-T2. (C) Western blots of SERCA 2b and ERp57 from lysates of experimental oocytes. One oocyte equivalent was loaded per lane and proteins were resolved through 12% SDS-PAGE. Gels represent three independent Western blots. (D) In vitro translations of ERp57 and mutants in rabbit reticulocytes in the absence or presence of canine pancreatic microsomes. Note that the signal peptide was proteolytically cleaved in reactions supplemented with microsomes. This gel is representative of four independent experiments. Bar, 100 μm.

ERp57 catalytic activity correlates with the reduction in SERCA 2b activity

To determine the relationship between ERp57 catalytic activity with Ca^{2+} pump activity, we coexpressed wild-type or mutant ERp57 with SERCA 2b. As expected, ERp57 had the highest effect in reducing the frequency of Ca^{2+} oscillations (i.e., reduced pump activity). The ERp57-T2 mutant that had 70% enzymatic activity in the insulin assay exhibited intermediate levels of pump inhibition. Neither ERp57-T1 (30% enzyme activity) nor ERp57-T1T2 (devoid of enzyme activity) affected the Ca^{2+} wave period and $t_{1/2}$ that was enhanced by SERCA 2b overexpression (Fig. 4, A and B). Western blots demonstrated that ERp57 and its mutants as well as SERCA 2b expression levels were similar throughout expression groups (Fig. 4 C). Independent confirmation that all ERp57 mutants were correctly processed in the ER was provided by in vitro translations supplemented with canine microsomes (Fig. 4 D). Together, these results strongly suggest that ERp57 oxidoreductase activity is responsible for the modulation of Ca^{2+} uptake by SERCA 2b.

The interaction between ERp57 and L4 is specific and Ca^{2+} dependent

To investigate the interaction between ERp57 and its potential target L4, we performed an in vitro GST pull-down experiment under various Ca^{2+} concentrations: the highest being 300 μM to mimic full Ca^{2+} store content and the lowest being 10 μM to mimic Ca^{2+} store depletion. Interestingly, ERp57 binds to L4 in a Ca^{2+}-dependent manner: the interaction is strongest at high Ca^{2+} (300 μM) and is significantly reduced at low Ca^{2+} (10 μM; Fig. 5 A). To test the specificity of this interaction we performed a similar GST pull-down experiment with GST-PDI. Neither GST-PDI nor GST alone interacted with the L4 (Fig. 5 B). This suggests that the interaction between ERp57 and L4 is specific. Moreover, this interaction occurs preferentially at high Ca^{2+} concentrations that are indicative of full Ca^{2+} stores (Pozzan et al., 1994).

Translational scanning studies of SERCAs indicate that they have intrinsic sequences that determine topologic insertion into the ER membrane (Bayle et al., 1995, 1997). To ascertain that the L4 construct was correctly inserted into the ER, a GFP-L4 fusion construct was coexpressed in *Xenopus* oocytes with a marker for ER localization, a DsRed-IP_3R fusion protein. As a control, cytosolic GFP was also coexpressed with DsRed-IP_3R. As expected, GFP-L4 colocalized with the IP_3R, whereas GFP had a more diffused cytosolic expression pattern (Fig. 5 C). These data indicate that the L4 construct was correctly localized in the ER.

ERp57 and PDI catalytic activity lack Ca^{2+} dependence

Because the association of ERp57 with the L4 substrate is stronger at higher Ca^{2+} concentrations, we tested whether the intrinsic activity of ERp57 is Ca^{2+} dependent. We measured in vitro the catalytic activity of purified GST-ERp57 at the same range of [Ca^{2+}] used in the GST pull-down assay (300, 150, 50, and 10 μM). The activity of ERp57 was only mildly but not significantly dependent on Ca^{2+} at the concentrations measured (Fig. 6 A). A similar assay was also performed for GST-PDI and in this case we found no Ca^{2+} dependence of its activity (Fig. 6 B).

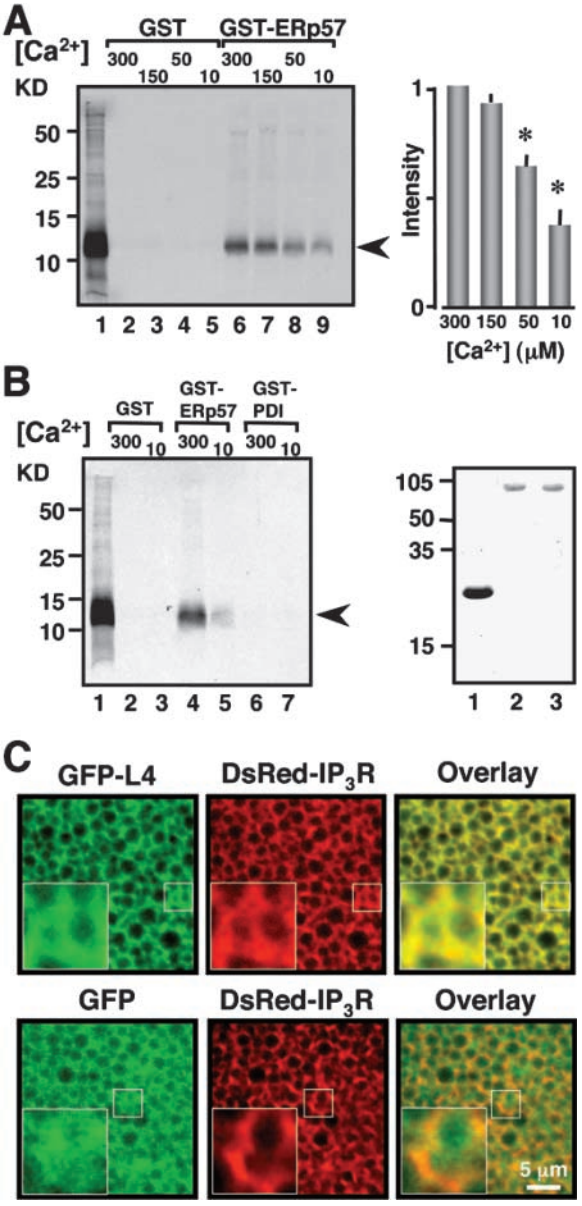

Figure 5. **The interaction between ERp57 and L4 is Ca^{2+} dependent and specific.** (A) GST pull-down assays performed at the indicated [Ca^{2+}] in micromolars. The gel is loaded as follows: input of in vitro–translated L4 (lane 1); pull downs for 30 μg GST control (lanes 2–5); pull downs for 10 μg GST-ERp57 (lanes 6–9). Proteins were resolved through 15% SDS-PAGE. L4 migrates ~11 kD (109 aa). Data represent three independent experiments. Histogram depicts densitometric analysis from these experiments. L4 bands were normalized to the intensity of the band at 300 μM Ca^{2+}. Asterisks indicate statistical significance ($P < 0.05$, one-way ANOVA). (B) The interaction between ERp57 and L4 is specific by GST pull-down assay. Lanes were loaded as follows: input of in vitro–translated L4 (lane 1); 30 μg GST negative control at the indicated [Ca^{2+}] (lanes 2 and 3); 10 μg GST-ERp57 (lanes 4 and 5); 10 μg GST-PDI (lanes 6 and 7). Proteins were resolved through 15% SDS-PAGE. The gel represents three independent experiments. (Right gel) Coomassie blue stain of 3 μg purified GST (lane 1); 1 μg GST-ERp57 (lane 2), and 1 μg GST-PDI (lane 3). Proteins were resolved through 13% SDS-PAGE. GST migrates ~27 kD, and GST-ERp57 and GST-PDI migrate ~80 kD (mature rPDI is 489 aa, mature hERp57 is 481 aa). The arrowheads correspond to L4. (C) The L4 protein localizes to the ER. (Top) Coexpression in *Xenopus* oocytes of GFP-L4 (green) with DsRed-IP_3R (red). The IP_3R is used as a marker of ER localization. The overlay (yellow) demonstrates that the L4 localizes in the ER. (Bottom) Cytosolic GFP (green) used a negative control, is coexpressed with DsRed-IP_3R (red). Note that the cytosolic GFP expression pattern is more diffused than that of the GFP-L4 and that there is no overlap of the two proteins indicating lack of colocalization. High magnification of the small square regions are shown as insets in each figure. Bar, 5 μm.

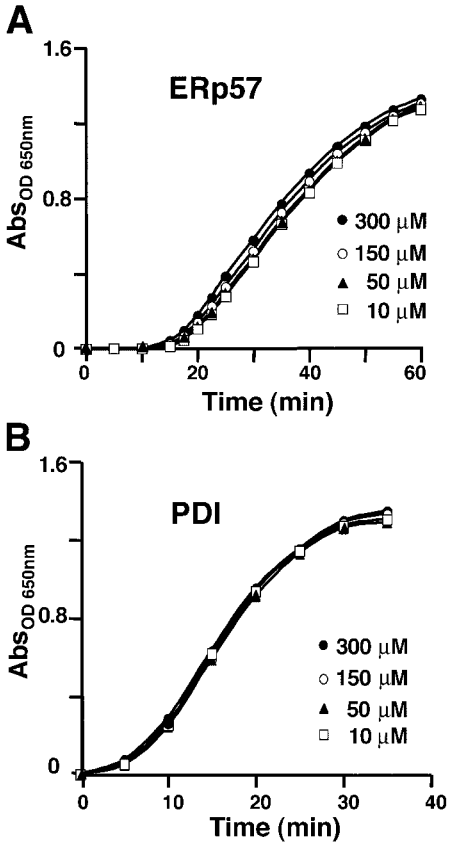

Figure 6. **The catalytic activity of ERp57 and PDI is Ca^{2+} independent.** Enzymatic activity is measured using the insulin turbidity assay at the indicated Ca^{2+} concentrations. $Absorbance_{OD\,650}$ values were collected in triplicate and plotted. These plots represent four independent experiments. The standard error bars were smaller than the size of the symbols. Input amounts of GST-ERp57 and GST-PDI fusion proteins was 0.8 μM.

The effects of ERp57 on Ca^{2+} wave activity are specific for the SERCA 2b isoform

CRT and CLNX inhibit Ca^{2+} oscillations via an interaction with the COOH-terminal sequence of SERCA 2b where a glycosylation consensus motif exists (John et al., 1998; Roderick et al., 2000). Furthermore, CRT does not interact with SERCA 2a, which lacks the 11th transmembrane segment and a COOH terminus in the ER lumen (John et al., 1998). ERp57 binds to CRT's P domain (Zapun et al., 1998; Oliver et al., 1999; Frickel et al., 2002; Leach et al., 2002). Based on these observations, we hypothesized that CRT binds the COOH-terminal sequence of the pump and recruits ERp57 to modulate L4 thiol groups and consequently pump activity. Because SERCA 2a also has the L4, we tested whether ERp57 modulates SERCA 2a directly or whether

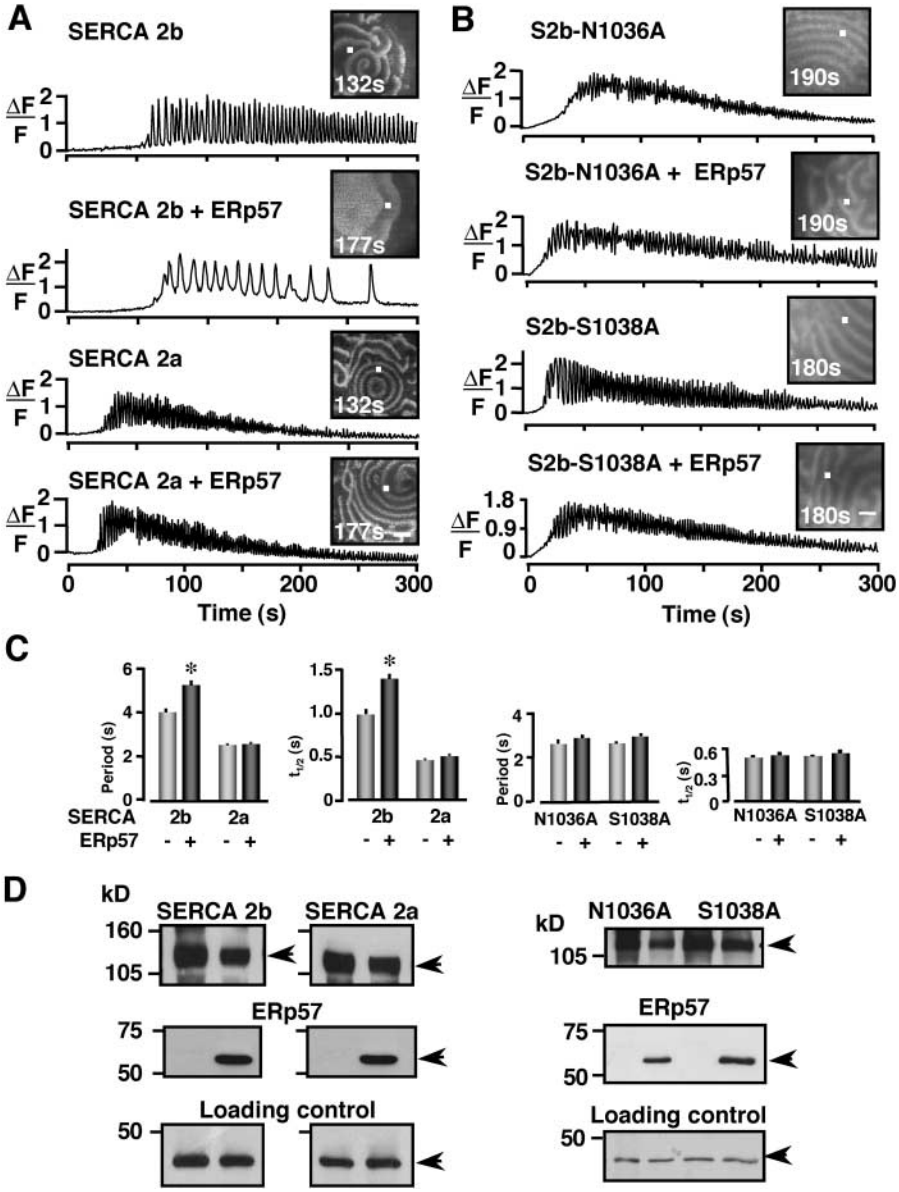

Figure 7. **ERp57 does not affect Ca^{2+} oscillations mediated by SERCA 2a, nor SERCA 2b glycosylation motif mutants.** (A) Confocal images of Ca^{2+} oscillations in oocytes overexpressing SERCA 2b ($n = 31$), SERCA 2b + ERp57 ($n = 39$), SERCA 2a ($n = 25$), and SERCA 2a + ERp57 ($n = 30$). The traces represent two independent experiments with 12–20 oocytes per group. (B) Images of Ca^{2+} oscillations in oocytes overexpressing SERCA 2b-N1036A ($n = 34$), SERCA 2b-N1036A + ERp57 ($n = 15$), SERCA 2b-S1038A ($n = 37$), and SERCA 2b-S1038A + ERp57 ($n = 16$). The traces represent two independent experiments with 8–19 oocytes per group. (C) Histograms plot period and $t_{1/2}$ for experiments in A and B, respectively. Asterisks indicate statistical significance ($P < 0.05$, *t* test) between SERCA 2b with SERCA 2b + ERp57 oocytes. (D) Western blots of SERCA 2a, SERCA 2b, or its mutants, and ERp57 from lysates of experimental oocytes as labeled. One oocyte equivalent was loaded per lane and proteins were resolved through 12% SDS-PAGE. Arrowheads indicate the protein as labeled at the top of each gel Bars: (A and B) 100 μm.

the effects are specific to SERCA 2b via CRT. We coexpressed ERp57 with SERCA 2a and found that ERp57 does not modulate Ca^{2+} oscillations in oocytes overexpressing this pump isoform (Fig. 7 A). We also coexpressed ERp57 with two mutants that eliminated the consensus glycosylation motif in SERCA 2b (SERCA 2b-N1036A and SERCA 2b-S1038A). We find that ERp57 does not modulate Ca^{2+} oscillations mediated by these two pump mutants (Fig. 7 B). Histograms of period and $t_{1/2}$ are shown in Fig. 7 C, whereas Western blots for these experiments are shown in Fig. 7 D. Together, these experiments demonstrate that CRT is required to recruit ERp57 to the L4.

Mechanism of ERp57 modulation of Ca^{2+} oscillations

The globular domain of CRT comprises the N and C domains and interacts with substrate glycoproteins, whereas the tip of the P domain binds to ERp57 and promotes disulfide bond formation (Ellgaard et al., 2001, 2002; Schrag et al., 2001; Frickel et al., 2002; Leach et al., 2002). Previous observations from our group demonstrated that CRT-NP (i.e., CRT lacking the C domain) modulated SERCA 2b just like wild-type CRT, indicating that in this case the C domain might not be necessary for the interaction (Camacho and Lechleiter, 1995; John et al., 1998). Thus, CRT most likely targets the COOH-terminal sequence of SERCA 2b via its N domain, whereas the P domain recruits ERp57 to interact with the L4. To test this hypothesis, we overexpressed four dominant negative constructs (L4, CRT-NC, CRT-N, or CRT-P) to determine whether they would interrupt the interaction between endogenous SERCA 2b with the ERp57–CRT complex. We found that oocytes overexpressing these four constructs exhibited shorter $t_{1/2}$ values (faster SERCA 2b activity) than control oocytes. In contrast, oocytes overexpressing CRT or CRT-NP exhibited longer $t_{1/2}$ values, consistent with previous findings (Camacho and Lechleiter, 1995; John et al., 1998; Fig. 8).

To determine the specificity of these dominant negative constructs for SERCA 2b, we also coexpressed them with ei-

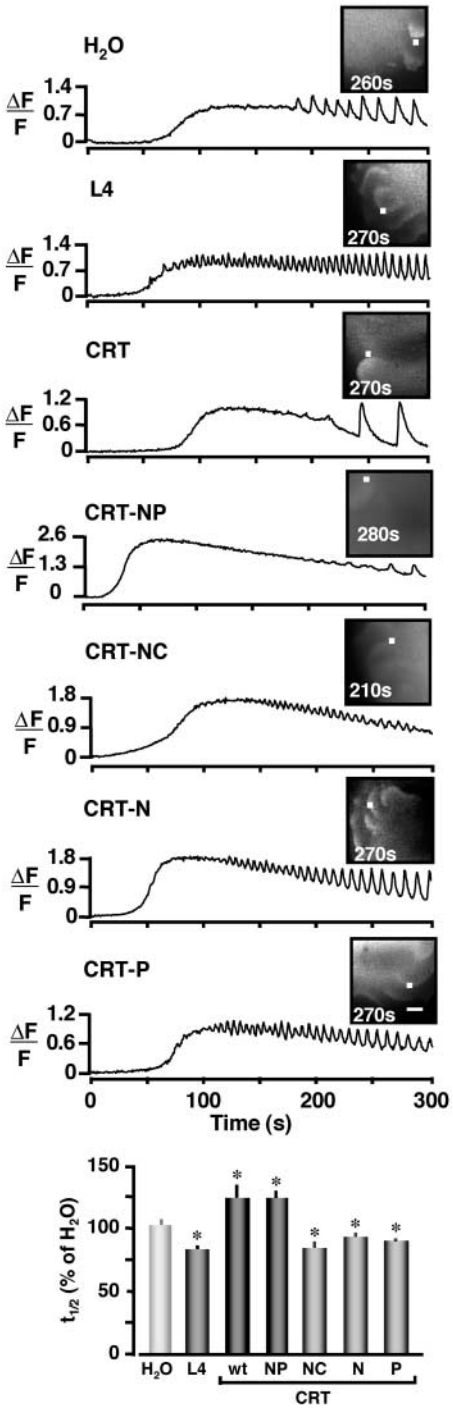

Figure 8. **Overexpression of L4, NC, N, or P domains of CRT increase Ca^{2+} oscillation frequency.** Representative confocal images of Ca^{2+} oscillations in oocytes as labeled: H_2O ($n = 46$); L4 ($n = 31$); CRT ($n = 22$); CRT-NP ($n = 28$); CRT-NC ($n = 28$); CRT-N domain ($n = 45$); and CRT-P domain ($n = 49$). Two independent experiments with 11–25 oocytes per group were performed. Histogram plots $t_{1/2}$ of individual waves normalized to the H_2O control group. Asterisks indicate statistical significance ($P < 0.05$, *t* test) between L4, CRT, CRT-NP, CRT-NC, CRT-N, CRT-P, and the control group. Bar, 100 μm.

ther SERCA 2a or SERCA 2b. Oocytes coexpressing L4, CRT-NC, CRT-N, or CRT-P with SERCA 2b exhibited significantly shorter $t_{1/2}$ values than SERCA 2b overexpressing oocytes, consistent with our observations presented in the previous paragraph. Note that control oocytes coexpressing CRT with SERCA 2b exhibited the longest $t_{1/2}$ values (lowest frequency of Ca^{2+} oscillations; Camacho and Lechleiter, 1995; Fig. 9, A and B). In agreement with the results reported in Fig. 7, we found that Ca^{2+} oscillations enhanced by SERCA 2a were not affected by coexpression with these constructs (Fig. 9 C). Together, these data support our model that CRT recruits ERp57 to the lumenal L4 in SERCA 2b, modulating pump activity to maintain ER Ca^{2+} homeostasis (Fig. 10).

Discussion

It is well established that CRT or CLNX form a macromolecular complex with ERp57 to assist in glycoprotein folding. In particular, CRT interacts with targeting glycoproteins via its globular domain, whereas the tip of the P domain recruits ERp57 to the glycoprotein substrate to promote intra/inter disulfide bond formation (High et al., 2000; Ellgaard et al., 2001, 2002; Schrag et al., 2001, 2003; Frickel et al., 2002; Leach et al., 2002; Ellgaard and Helenius, 2003; Kostova and Wolf, 2003). From our work using the Ca^{2+} oscillation assay in *Xenopus* oocytes, we have found that both the N and P domains of CRT are necessary for inhibition of Ca^{2+} oscillations enhanced by SERCA 2b, whereas the C domain is not required (Camacho and Lechleiter, 1995; John et al., 1998; Roderick et al., 2000). In this paper, we are led to the conclusion that CRT uses the N domain to target the COOH-terminal sequence of SERCA 2b, and the P domain to recruit ERp57 to interact with the L4 of SERCA 2b. Several of our findings support this conceptual model. ERp57 does not affect Ca^{2+} oscillations enhanced by SERCA 2a, nor SERCA 2b mutants defective in the COOH-terminal glycosylation motif. Overexpression of L4 or the NC, N, or P domains of CRT exhibit dominant negative effects that presumably act by disrupting the interaction between the endogenous CRT–ERp57 complex and SERCA 2b. In particular, overexpression of the first construct, L4, should bind endogenous ERp57 preventing it from regulating the pump. The second construct, CRT-NC, contains the entire globular domain that binds the glycosylated NFS motif of SERCA 2b, but lacks the ability to recruit ERp57 (Schrag et al., 2001; Leach et al., 2002). Its overexpression should compete with the interaction of endogenous CRT with SERCA 2b, thereby preventing ERp57 from regulating pump activity. The third construct, CRT-N, contains two residues that are responsible for binding glucose (Schrag et al., 2001). Its overexpression has the same effect as CRT-NC, indicating that this construct is sufficient to target the SERCA 2b COOH-terminal sequence. The fourth construct, CRT-P, contains the repeat known as 1112, which is longer than the fragment used by Ellgaard and colleagues (Ellgaard et al., 2002), who found that a shorter fragment (repeat 112) was sufficient to interact with ERp57. Without the globular NC domain, the P domain itself is unable to target the glycan (Leach et al., 2002). Consequently, overexpression of CRT-P should bind endogenous ERp57 and prevent regulation of SERCA 2b.

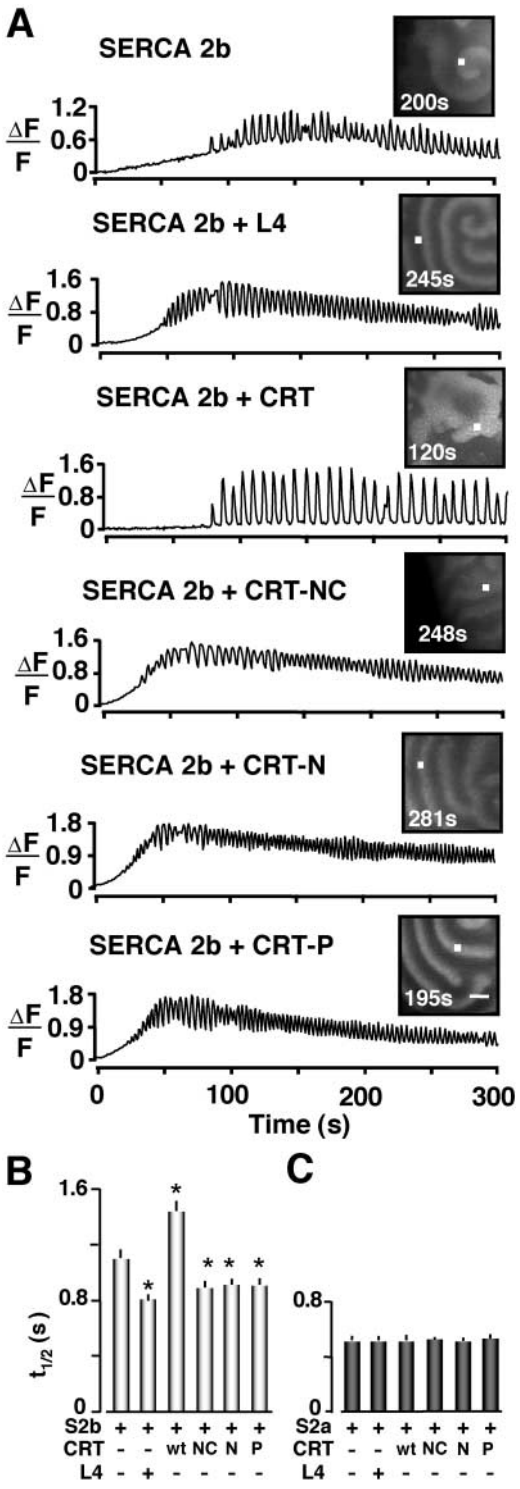

Figure 9. **Dominant negative constructs increase the frequency of Ca^{2+} oscillations enhanced by SERCA 2b, but not SERCA 2a.** (A) Confocal images of Ca^{2+} oscillations in *Xenopus* oocytes overexpressing SERCA 2b ($n = 22$); or coexpressing SERCA 2b with L4 ($n = 22$); CRT ($n = 22$); CRT-NC ($n = 21$); CRT-N ($n = 21$); and CRT-P ($n = 21$) are shown. Two independent experiments with 10–11 oocytes per group were performed. (B) Histogram plots $t_{1/2}$ of individual waves. Asterisks indicate statistically significant difference ($P < 0.05$, *t* test) between L4, CRT, CRT-NC, CRT-N, and CRT-P with respect to the SERCA 2b (S2b) overexpression. (C) Histogram shows the result of a similar experiment performed for SERCA 2a. Confocal images of Ca^{2+} oscillations in oocytes overexpressing SERCA 2a ($n = 21$) or coexpressing SERCA 2a with L4 ($n = 20$); CRT ($n = 20$); CRT-N ($n = 20$); CRT-P ($n = 20$); and CRT-NC ($n = 20$) are not depicted. Note that on the same y-axis scale as in experiment in B, none of the tested constructs display a significant difference with respect to SERCA 2a (labeled S2a). Bar, 100 μm.

ERp57 and its homologue PDI have different substrate specificities (Freedman et al., 2002; Clissold and Bicknell, 2003). ERp57 specifically associates with N-linked glycoproteins, whereas PDI does not. This specificity is mainly mediated by an interaction with CRT or CLNX (Oliver et al., 1997, 1999; Van der Wal et al., 1998; Zapun et al., 1998; High et al., 2000; Frickel et al., 2002). Using in vitro GST pull-down experiments, we also demonstrated that ERp57 specifically interacts with the L4 of SERCA 2b, whereas PDI did not. It is possible that there is a direct interaction between ERp57 and L4, but it is equally likely that an indirect protein interaction is occurring in a pull-down assay. For example, microsomes contain CRT and glycoproteins (e.g., SERCA 2b), which could then link ERp57 to L4. In fact, the bulk of our results favor the requirement of CRT to recruit ERp57 to the L4.

The mechanisms that regulate SERCA activity from the ER have been until now somewhat unclear. Decreased lumenal Ca^{2+} induces a strong stimulation of SERCA activity in isolated pancreatic acinar cells (Mogami et al., 1998). We demonstrate that the association of ERp57 with the L4 is Ca^{2+} dependent in the physiological range of ER lumenal Ca^{2+} (10, 50, 150, and 300 μM). The Ca^{2+} dependency of the association between ERp57 and L4 is likely to be mediated by CRT, because Ca^{2+} does not regulate the intrinsic enzyme activity of the ERp57. It has been reported that Ca^{2+} is required for CRT binding to oligosaccharides, although these experiments were conducted beyond physiological [Ca^{2+}] (10 mM Ca^{2+}; Vassilakos et al., 1998). Ca^{2+} has also been shown to modulate the interaction between CRT and ERp57 (Corbett et al., 1999). Together, our data suggest the following role of ER Ca^{2+} in the feedback mechanism that regulates SERCA 2b activity (Fig. 10). When ER Ca^{2+} stores are full (~300 μM Ca^{2+}), ERp57 binds to L4 promoting disulfide bond formation in the loop, which inhibits pump activity. When Ca^{2+} stores become depleted (~10 μM Ca^{2+}), ERp57 dissociates from L4, resulting in the reduced form of SERCA 2b that is more active. The mechanism by which thiol groups in the L4 are reduced after ERp57 dissociates from the pump is unknown. The ER lumen maintains a neutral to slightly oxidized environment (GSH–GSSG ~1–3; Hwang et al., 1992). Our results suggest that ERp57 must be bound to L4 in order to maintain it in an oxidized state. It is possible that additional ER proteins play a role here. Regardless of the precise underlying mechanism, our data clearly indicate that the reduced form of L4 supports higher pump activity to rapidly refill the ER.

The CLNX–CRT cycle has a well-established role in productive glycoprotein folding and quality control of nascent glycoproteins undergoing folding (High et al., 2000; Ellgaard and Helenius, 2003; Kostova and Wolf, 2003; Schrag et al., 2003). Our observations indicate that these ER chaperones interact with a mature ER resident glyco-

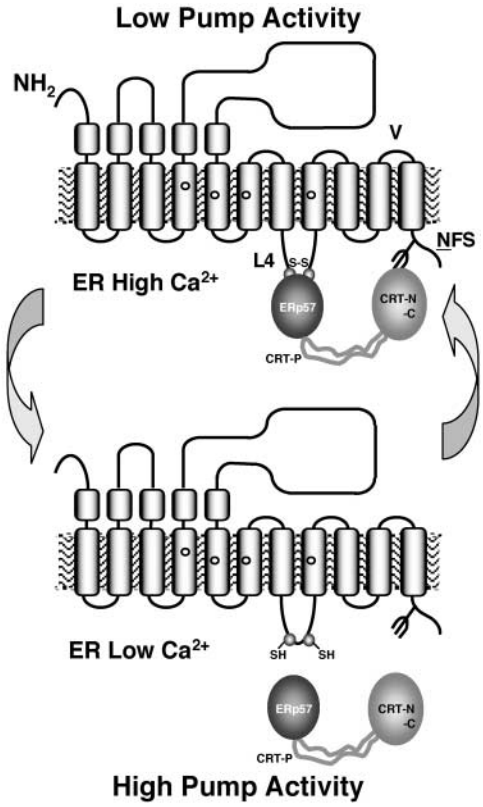

Figure 10. **Model depicting the functional consequences of the interaction between ERp57–CRT with SERCA 2b.** At rest, the ER Ca^{2+} stores are full (high $[Ca^{2+}]_{ER}$), the N domain of CRT interacts with the COOH-terminal sequence of SERCA 2b, whereas the P domain recruits ERp57 to target L4 in SERCA 2b. At high $[Ca^{2+}]_{ER}$ our data suggest that ERp57 promotes disulfide bond formation between thiol groups in the loop, reducing pump activity (i.e., decreasing the frequency of Ca^{2+} oscillations and $t_{1/2}$). This activity of ERp57 favors disulfide bond formation because the prevailing conditions in the ER are relatively oxidizing. As $[Ca^{2+}]_{ER}$ decreases below ~50 μM, ERp57 dissociates from L4, allowing SERCA 2b in its reduced form (cysteine mutagenesis) to be more active. Thus, at low $[Ca^{2+}]_{ER}$ SERCA 2b favors ER store refilling. The arrow indicates the point of divergence between SERCA 2a and SERCA 2b. NFS is the glycosylation consensus motif at the COOH-terminal sequence of SERCA 2b.

protein (SERCA 2b). Association/dissociation of other ER chaperones with mature proteins has also been reported during the unfolded protein response (Bertolotti et al., 2000). We speculate that the classical CLNX–CRT cycle and the system we have characterized here exist in parallel and that the action of CRT–CLNX on SERCA 2b provides the homeostatic feedback necessary to maintain Ca^{2+} conditions that promote productive glycoprotein folding. Without it, Ca^{2+} depletion could result in the well-known unfolded protein response, which can bring about cellular apoptosis under certain stress conditions (Kaufman, 1999; Welihinda et al., 1999; Patil and Walter, 2001; Harding et al., 2002). Maintaining optimal Ca^{2+} concentrations in the ER is clearly important for nascent protein folding (Hardman and Wetmore, 1996; Chen et al., 1997; Stevens and Argon, 1999; Ramsden et al., 2000). The ability of the lectin chaperones to "talk" to a mature protein in the Ca^{2+} signaling machinery provides the mechanism by which the optimal Ca^{2+} environment is maintained for protein folding.

Oxidant treatment inactivates SERCA 2b to a greater extent than other pump isoforms (Grover et al., 1997; Barnes et al., 2000). Our observations imply that SERCA 2b is in fact a redox sensor. In the oxidized state of L4, this pump exhibits lower activity. On the other hand, the pump favors rapid Ca^{2+} uptake in the L4 mutants that are constitutively reduced by cysteine mutagenesis. Interestingly, the ryanodine receptor, a Ca^{2+} release channel located on the SR–ER is also a redox sensor (Zable et al., 1997; Xia et al., 2000; Sun et al., 2001). The oxidized channel correlates with the open state, whereas the reduced form correlates with channel closure. The IP_3R may also sense the redox potential because it contains cysteines in the ER lumenal facing loop that line the channel pore. Consequently, modulation of redox potential of reactive thiols in the ER might be a general mechanism by which SERCA 2b, IP_3R, and ryanodine receptor control ER Ca^{2+}. In terms of Ca^{2+} homeostasis, our observations with ERp57 fit the view that ER redox modulates Ca^{2+} release and uptake in coordinate and opposite directions. In particular, oxidization appears to favor Ca^{2+} release by opening Ca^{2+} channels and inhibiting Ca^{2+} pumping. On the other hand, reduction seems to favor Ca^{2+} uptake by channel closure and increasing Ca^{2+} pumping. The combined effect of these two actions helps to minimize the loss of ER Ca^{2+} and maximize refilling of the stores, thereby protecting the physiological functions of the ER such as glycoprotein folding.

Materials and methods

Vectors and reagents

The *Xenopus* expression vectors for rat SERCA 2a and SERCA 2b have been described previously (John et al., 1998). L4 cysteine–deficient mutants of SERCA 2b were generated as follows: cysteines 875 and 887 were mutated to serines (mutant SERCA 2b-C1SC2S) or to alanines (mutant SERCA 2b-C1AC2A). A two-step mutagenesis protocol was performed. To generate the SERCA 2b-C1SC2S mutation primers 5′-GCTGAGTCATTTCCTGCAGTCAAAGGAGGACAACCC-3′ and 5′-CCAGACTTCGAAGGAGTGGATTCAGCAATCTTTGAGTCCC-3′ with their respective reverse complement primers were used. Primers 5′-GCTGAGTCATTTCCTGCAGGCTAAGGAGGACAACCC-3′ and 5′-CCAGACTTCGAAGGAGTGGATGCTGCAATCTTTGAGTCCC-3′ and their respective reverse complement primers were used for the SERCA 2b-C1C2A mutant. Plasmid pHN-SERCA 2b-C875G was generated using the forward primer 5′-GCTGAGTCATTTCCTGCAGGGTAAGGAGGACAACCC-3′ and its reverse complement. Plasmid pHN-SERCA 2b-N1036A has been generated and published previously (John et al., 1998). Mutant SERCA 2b-S1038A (plasmid pHN SERCA 2b-S1038A) was generated by PCR using the forward primer 5′-AGCACAGACACTAACTTTGCTGATATGTTCTGG-3′ and the reverse primer 5′-CCAGAACATATCAGCAAAGTTAGTGTCTGTGCT-3′.

A construct encoding the L4 of SERCA 2b was generated by PCR amplification spanning methionine 814 and arginine 922 with primers 5′-ACTGGGATCCATGAACAAACCCCCACGGAACCCA-3′ and 5′-ACTGAAGCTTTTACCTCAGCAGGGACTGGTTTTC-3′. The PCR product was ligated into the BamHI and HindIII sites of the similarly digested vector pHN (plasmid pHN-SERCA 2b-L4). To generate plasmid pHN-GFP-L4, a BamHI fragment from pHN-GFP-S65T-ΔTAA, as described previously (John et al., 1998), was subcloned into plasmid pHN-SERCA 2b-L4 that was digested with BamHI and treated with calf intestinal phosphatase. Plasmid pHN-GFT S65T was generated previously (John et al., 1998). The *Xenopus* expression vector of DsRed-IP_3R was generated by a three-step PCR protocol to create a fusion of DsRed to the NH_2-terminal sequence of the IP_3R. First, the full-length DsRed was amplified by PCR from the template of pDSRed 1-N1 (CLONTECH Laboratories, Inc.). The forward and reverse primers were 5′-ACTGGAATTCATGGTGCGCTCCTCCAAGAACGTC-3′ and 5′-AAGAAAGCTGGACATTTCATTCATCAGGAACAGGTGGTGGCGGCC-3′. Second, the NH_2

terminus of IP_3R was amplified by PCR from template pHN-IP_3R with the forward and reverse primers as 5′-GGCCGCCACCACCTGTTCCTGATGAATGAAATGTCCAGCTTTCTT-3′ and 5′-GTGCACATGTAGCATCAGGTGGCAGAATGA-3′. The purified PCR products served as templates to create the final product DsRe-IP_3R. In this PCR reaction, the forward and reverse primers were 5′-ACTGGAATTCATGGTGCGCTCCTCCAAGAACGTC-3′ and 5′-GTGCACATGTAGCATCAGGTGGCAGAATGA-3′. The final PCR fusion product was digested with EcoRI and NsiI and subcloned into the EcoRI and NsiI sites of PHN-IP_3R.

The *Xenopus* expression vector of ERp57 (plasmid pHN-ERp57) was generated in a three-step PCR protocol. First, the mature human ERp57 was amplified from the template pET9-ERp613 (a gift from D.Y. Thomas, Biotechnology Research Institute, Montréal, Canada) with primers 5′-CTGCTCGGCCTGGCCGCCGCCTCCGACGTGCTAGAACTCACG-3′ and 5′-ACGTAAGCTTTTAGAGATCCTCCTGTGCCTTCTT-3′. A second PCR generated the signal peptide of CRT from the template pHN-CRT (Camacho and Lechleiter, 1995) using primers 5′-TAATACGACTCACTATAGGG-3′ and 5′-CGTGAGTTCTAGCACGTCGGAGGCGGCGGCCAGGCCGAGCAG-3′. The purified PCR products served as templates to generate a fusion of the CRT signal peptide and mature ERp57. In this PCR reaction, the forward and reverse primers were 5′-TAATACGACTCACTATAGGG-3′ and 5′-ACGTAAGCTTTTAGAGATCCTCCTGTGCCTTCTT-3′. The final PCR fusion product was subcloned into the HindIII and SSTI sites of the *Xenopus* expression vector pHN. Three mutants of ERp57 were generated. The first mutant had cysteines 57 and 60 mutated to serines in the NH_2-terminal thioredoxin motif (mutant ERp57-T1) and was generated by PCR using primer 5′-CGAGTTCTTCGCTCCCTGGTCTGGACACTCCAAGAGACTTGCACC-3′ and its reverse complement. The second construct had cysteines 406 and 409 in the COOH-terminal thioredoxin motif mutated to serines (mutant ERp57-T2) and was generated using primer 5′-GAATTTTATGCCCCTTGGTCTGGTCATTCTAAGAACCTGGAGCCC-3′ and its reverse complement. The third construct was a double mutant generated in two PCR steps with the above primers (mutant ERp57-T1T2).

Rat PDI cDNA was cloned from a rat liver cDNA library (Invitrogen) by PCR using primers 5′-ACTGGGATCCATGCTGAGCCGTGCTTTGCTGTGC-3′ and 5′-ACTGTCTAGACTACAGTTCATCCTTCACGGC-3′ based on the GenBank/EMBL/DDBJ accession no. X02918. The PCR product was subcloned into the BamHI and XbaI sites of pHN and fully sequenced.

To obtain GST-ERp57 fusion proteins including wild type and mutants as well as GST-PDI, we amplified the corresponding mature cDNA fragments by PCR and subcloned them into pGEX-4T-2 vector (Amersham Biosciences). For ERp57 and its mutants, the primers were 5′-TCGAGGATCCATGTCCGACGTGCTAGAACTCACG-3′ and 5′-ACTGCTCGAGTTAGAGATCCTCCTGTGCCTTCTT-3′, whereas for PDI, the primers were 5′-ACTGGGATCCATGGACGCTCTGGAGGAGGAGGAC-3′ and 5′-ACTGCTCGAGCTACAGTTAATCCTTCACGGC-3′. The PCR products were ligated into the BamHI and XhoI sites of pGEX-4T-2.

The *Xenopus* vectors encoding CRT, CRT-NP, CRT-NC, and CRT-N domains have been published previously (Camacho and Lechleiter, 1995). The construct for expression of the P domain (plasmid pHN-CRT-P) was generated by PCR mutagenesis designed to remove the N domain from template pHN-CRT-NP (Camacho and Lechleiter, 1995). The primers used had sequence 5′-GCCGCCGAGCCCGATGACTGGGACTTCCTACCCCCCAAGAAGATAAAGGACCCA-3′ and 5′-TGGGTCCTTTATCTTCTTGGGGGGTAGGAAGTCCCAGTCATCGGGCTCGGCGGC-3′. The resulting construct contains the CRT signal peptide followed by the P domain (amino acids 181–260) and a KDEL sequence for ER retention.

Automatic sequencing of all cDNA constructs was performed at the UTHSCSA Advance Nucleic Acid Core Facility. All primers were purchased from Operon Technologies (QIAGEN). Unless otherwise specified, all chemicals were purchased from Sigma-Aldrich and all restriction enzymes were purchased from Invitrogen Life Technologies.

In vitro transcriptions and translations

Synthetic mRNA was prepared as described previously (Camacho and Lechleiter, 1995). In vitro translations were performed as described previously (Roderick et al., 2000).

Western blots

Oocytes extracts were prepared as described previously (Camacho and Lechleiter, 1995). In brief, 5–10 oocytes were pooled and homogenized in buffer containing 20 mM Tris-HCl, pH 7.6, 140 mM NaCl, 250 mM sucrose, and protease inhibitors in a mix containing 0.2 mM AEBSF, 10 μM leupeptin, 1 μM pepstatin A, and 0.8 mM benzamidine (Calbiochem). After centrifugation at 4,500 *g* for 15 min at 4°C, the supernatant was ultracentrifuged at 125,000 *g* for 20 min at 4°C. Microsomal pellets were resuspended in solubilization buffer (10 mM Tris-HCl, pH 7.6, 140 mM NaCl, 1% Triton X-100, and protease inhibitors). A second centrifugation (15,000 *g* for 10 min) was performed to discard the insoluble material. SDS-PAGE was performed by loading 1–2 oocyte equivalents per lane and transferred to nitrocellulose. A polyclonal rabbit anti-SERCA antibody (NI, 1:8,000 dilution, a gift from J. Lytton, University of Calgary, Calgary, Canada) was used to detect SERCA 2b. A rabbit anti-ERp57 polyclonal antibody (1:4,000 dilution, a gift from S. High, University of Manchester, Manchester, UK) was used to detect ERp57. HRP-conjugated donkey anti–rabbit IgG secondary antibodies (Jackson ImmunoResearch Laboratories) in a dilution of 1:10,000 were used in all Western blots and visualized by ECL (PerkinElmer Life Sciences, Inc.).

GST fusion protein purification

BL21 bacteria transformed with pGEX-4T-2, pGEX-4T-2-PDI or pGEX-4T-2-ERp57 (and mutants) were grown to OD 600 nm 0.6. Isopropyl-β-D-thiogalactopyranoside (Research Products International Corp.) was added to a final concentration of 1 mM to induce protein expression for 4 h at 37°C. Bacteria were lysed by sonication in 1× PBS containing 100 mM EDTA and a mix of protease inhibitors including (200 μM AEBSF, 10 μM leupeptin, and 1.5 μM pepstatin A) and 0.8 mM benzamidine. Bacterial lysates were centrifuged at 22,000 *g* and the supernatant collected. Binding of GST or GST fusion proteins to glutathione-Sepharose 4B (Amersham Biosciences) was performed at 4°C for 1 h followed by three washes with equilibration buffer (0.5 M Tris-HCl, pH 8.0, 4 mM EDTA, 0.1% β-ME, 5% glycerol). Elution of bound protein was performed in this buffer supplemented with 15 mM glutathione. Proteins were dialysed against 0.05 M Tris-HCl, pH 7.5, containing 1 mM EDTA, 0.2% β-ME, and stored at –80°C.

GST pull-down assays

In vitro translation of L4 was accomplished in a rabbit reticulocyte lysates supplement with canine pancreatic microsomes (both from Promega) and L-[^{35}S]methionine (PerkinElmer Life Sciences). Microsomes were isolated and resuspended in solubilization buffer (10 mM Tris-HCl, pH 7.6, 140 mM NaCl, 1% Triton X-100 and a mixture of the protease inhibitors described in Western blots). Binding of in vitro–translated L4 to GST-ERp57 fusion protein(s) was performed at 4°C overnight in the presence of glutathione Sepharose 4B (Amersham Biosciences) in binding solution containing in mM 10 Tris-HCl, pH 8.0, 70 KCl, 2 $MgCl_2$, 50 μM EGTA, 5% BSA, and protease inhibitors supplemented with experimental $CaCl_2$ concentrations (60, 100, 200, and 350 μM). Proteins bound to glutathione Sepharose beads were washed three times in buffer containing 0.2 M Tris-HCl, pH 8.0, 0.1% Triton X-100, 70 mM KCl, 2 mM $MgCl_2$, 50 μM EGTA, protease inhibitors, and corresponding $CaCl_2$ concentrations. Proteins were resolved by 15% SDS-PAGE and visualized by autoradiography. Ca^{2+} concentrations were calculated according to existing algorithms (Fabiato and Fabiato, 1979).

Insulin turbidity assay

The insulin turbidity assay was performed as described previously (Holmgren, 1979; Hirano et al., 1995). In this assay, oxidized insulin was used as substrate to measure thiol-dependent reductase activity of ERp57. Under reducing conditions, the two interchain disulphide bonds of insulin are cleaved, resulting in the formation of a white insoluble precipitate. 10 mg/ml of insulin (Sigma-Aldrich) stock solution was prepared as described previously (Holmgren, 1979). In brief, 100 mg of insulin was first resuspended in 8 ml 0.05 M Tris-HCl, pH 8.0. Subsequently, the pH was adjusted between 2.0 and 3.0 by adding 1 M HCl and rapidly titrated to pH 8.0 with 1 M NaOH. The final volume of the solution was adjusted to 10 ml with H_2O. The clear stock solution was stored at –20°C. On the experimental day, the insulin stock solution was diluted to 1 mg/ml with a buffer containing in 100 mM KAC, pH 7.5, and 2 mM EDTA, supplemented with $CaCl_2$ concentrations (2.44, 2.28, 2.17, and 2.12 mM) to yield free [Ca^{2+}] of 300, 150, 50, and 10 μM. The final reaction volume was adjusted to 1 ml after purified ERp57 or its mutants were added. The reaction was initiated by adding 3 μl of 100 mM DTT. $Abs_{650\ nm}$ was measured every 5 min in a BioSpec-1601 spectrophotometer (Shimadzu). Enzyme activity was defined by measuring the slope of the linear portion of the absorbance curve. Ca^{2+} concentrations were calculated according to known algorithms (Fabiato and Fabiato, 1979).

Oocyte methods and confocal imaging

Stage VI–defolliculated oocytes were injected a bolus of 50 nl of 1 μg mRNA using a standard positive pressure injector (Drummond Scientific). Oocytes were cultured in 50% L-15 media (Invitrogen) for 5–7 d at 18°C.

Intracellular Ca^{2+} was imaged as described previously (Roderick et al., 2000). Oocytes were injected with fluorescent Ca^{2+} indicator Oregon green II (12.5 μM final; Molecular Probes) 30–60 min before imaging. Ca^{2+} release was initiated by injecting a 50 nl bolus of 6 μM IP_3 (Calbiochem) to yield ~300 nM final concentration. Imaging was performed in ND96 buffer containing 1 mM EGTA. Images were acquired at a rate of 0.75 s /frame on a confocal laser scanning microscope (model PCM2000; Nikon) using a 10× objective (NA = 0.45) at zoom 1.

To characterize the ER localization of L4, GFP-L4 was coexpressed in oocytes with DsRed-IP_3R. Fluorescence was monitored using a confocal microscope (model Fluoview 500; Olympus). GFP-L4 as well as GFP (as a negative control) were detected using a 488-nm laser line for excitation and a combination of a 510-nm long pass and a 550-nm short pass barrier filter for signal emission. DsRed fluorescence was obtained with a 568-nm laser line for excitation and a 585-nm long pass barrier filter for emission. Emission signals were collected using a 60× oil (NA = 1.4) objective (Olympus) at zoom 5.

Imaging analysis

The analysis of Ca^{2+} images was performed using the public domain NIH ImageJ program (developed at the National Institutes of Health and available at http://rsb.info.nih.gov/ij/).

Statistical analysis

Statistical significance was determined by *t* test or one-way ANOVA as appropriate and accepted at $P < 0.05$.

We wish to thank David Y. Thomas for the cDNA encoding mature human ERp57, Stephen High for rabbit αERP57 antibody, and Johnathan Lytton for rabbit SERCA 2 antibody. We also thank James Lechleiter, Da-Ting Lin, and Marianna Bollo for critical reading of the manuscript.

This work was funded by National Institutes of Health grant R01 GM55372 to P. Camacho.

Submitted: 2 July 2003
Accepted: 25 November 2003

References

Ahn, W., M.G. Lee, K.H. Kim, and S. Muallem. 2003. Multiple effects of SERCA2b mutations associated with Darier's disease. *J. Biol. Chem.* 278: 20795–20801.

Antoniou, A.N., S. Ford, M. Alphey, A. Osborne, T. Elliott, and S.J. Powis. 2002. The oxidoreductase ERp57 efficiently reduces partially folded in preference to fully folded MHC class I molecules. *EMBO J.* 21:2655–2663.

Ashby, M.C., and A.V. Tepikin. 2001. ER calcium and the functions of intracellular organelles. *Semin. Cell Dev. Biol.* 12:11–17.

Barnes, K.A., S.E. Samson, and A.K. Grover. 2000. Sarco/endoplasmic reticulum Ca^{2+}-pump isoform SERCA3a is more resistant to superoxide damage than SERCA2b. *Mol. Cell. Biochem.* 203:17–21.

Bayle, D., D. Weeks, and G. Sachs. 1995. The membrane topology of the rat sarcoplasmic and endoplasmic reticulum calcium ATPases by in vitro translation scanning. *J. Biol. Chem.* 270:25678–25684.

Bayle, D., D. Weeks, S. Hallen, K. Melchers, K. Bamberg, and G. Sachs. 1997. In vitro translation analysis of integral membrane proteins. *J. Recept. Signal Transduct. Res.* 17:29–56.

Berridge, M.J., M.D. Bootman, and P. Lipp. 1998. Calcium–a life and death signal. *Nature.* 395:645–648.

Bertolotti, A., Y. Zhang, L.M. Hendershot, H.P. Harding, and D. Ron. 2000. Dynamic interaction of BiP and ER stress transducers in the unfolded-protein response. *Nat. Cell Biol.* 2:326–332.

Bouvier, M. 2003. Accessory proteins and the assembly of human class I MHC molecules: a molecular and structural perspective. *Mol. Immunol.* 39:697–706.

Camacho, P., and J.D. Lechleiter. 1993. Increased frequency of calcium waves in *Xenopus laevis* oocytes that express a calcium-ATPase. *Science.* 260:226–229.

Camacho, P., and J.D. Lechleiter. 1995. Calreticulin inhibits repetitive intracellular Ca^{2+} waves. *Cell.* 82:765–771.

Camacho, P., and J.D. Lechleiter. 2000. *Xenopus* oocytes as a tool in calcium signaling research. *In* Calcium Signaling. J.W. Putney, Jr., editor. CRC Press, Boca Raton, FL. 157–182.

Chen, L.B., S.K. Nigam, and G. Kuznetsov. 1997. Multiple molecular chaperones complex with misfolded large oligomeric glycoproteins in the endoplasmic reticulum. *J. Biol. Chem.* 272:3057–3063.

Clissold, P.M., and R. Bicknell. 2003. The thioredoxin-like fold: hidden domains in protein disulfide isomerases and other chaperone proteins. *Bioessays.* 25: 603–611.

Corbett, E.F., K. Oikawa, P. Francois, D.C. Tessier, C. Kay, J.J. Bergeron, D.Y. Thomas, K.H. Krause, and M. Michalak. 1999. Ca^{2+} regulation of interactions between endoplasmic reticulum chaperones. *J. Biol. Chem.* 274:6203–6211.

Dick, T.P., N. Bangia, D.R. Peaper, and P. Cresswell. 2002. Disulfide bond isomerization and the assembly of MHC class I-peptide complexes. *Immunity.* 16:87–98.

Dolmetsch, R.E., R.S. Lewis, C.C. Goodnow, and J.I. Healy. 1997. Differential activation of transcription factors induced by Ca^{2+} response amplitude and duration. *Nature*. 386:855–858. (published erratum in *Nature*. 1997. 388: 308)

Ellgaard, L., and A. Helenius. 2003. Quality control in the endoplasmic reticulum. *Nat. Rev. Mol. Cell Biol.* 4:181–191.

Ellgaard, L., R. Riek, T. Herrmann, P. Guntert, D. Braun, A. Helenius, and K. Wuthrich. 2001. NMR structure of the calreticulin P-domain. *Proc. Natl. Acad. Sci. USA.* 98:3133–3138.

Ellgaard, L., P. Bettendorff, D. Braun, T. Herrmann, F. Fiorito, I. Jelesarov, P. Guntert, A. Helenius, and K. Wuthrich. 2002. NMR structures of 36 and 73-residue fragments of the calreticulin P-domain. *J. Mol. Biol.* 322:773–784.

Fabiato, A., and F. Fabiato. 1979. Calculator programs for computing the composition of the solutions containing multiple metals and ligands used for experiments in skinned muscle cells. *J. Physiol. (Paris).* 75:463–505.

Falcke, M., Y. Li, J.D. Lechleiter, and P. Camacho. 2003. Modeling the dependence of the period of intracellular Ca^{2+} waves on SERCA expression. *Biophys. J.* 85:1474–1481.

Freedman, R.B., P. Klappa, and L.W. Ruddock. 2002. Protein disulfide isomerases exploit synergy between catalytic and specific binding domains. *EMBO Rep.* 3:136–140.

Frickel, E.M., R. Riek, I. Jelesarov, A. Helenius, K. Wuthrich, and L. Ellgaard. 2002. TROSY-NMR reveals interaction between ERp57 and the tip of the calreticulin P-domain. *Proc. Natl. Acad. Sci. USA.* 99:1954–1959.

Grover, A.K., S.E. Samson, and C.M. Misquitta. 1997. Sarco(endo)plasmic reticulum Ca^{2+} pump isoform SERCA3 is more resistant than SERCA2b to peroxide. *Am. J. Physiol.* 273:C420–C425.

Hajnoczky, G., E. Davies, and M. Madesh. 2003. Calcium signaling and apoptosis. *Biochem. Biophys. Res. Commun.* 304:445–454.

Harding, H.P., M. Calfon, F. Urano, I. Novoa, and D. Ron. 2002. Transcriptional and translational control in the mammalian unfolded protein response. *Annu. Rev. Cell Dev. Biol.* 18:575–599.

Hardman, K.D., and D.R. Wetmore. 1996. Roles of the propeptide and metal ions in the folding and stability of the catalytic domain of stromelysin (matrix metalloproteinase 3). *Biochemistry.* 35:6549–6558.

High, S., F.J. Lecomte, S.J. Russell, B.M. Abell, and J.D. Oliver. 2000. Glycoprotein folding in the endoplasmic reticulum: a tale of three chaperones? *FEBS Lett.* 476:38–41.

Hirano, N., F. Shibasaki, R. Sakai, T. Tanaka, J. Nishida, Y. Yazaki, T. Takenawa, and H. Hirai. 1995. Molecular cloning of the human glucose-regulated protein ERp57/GRP58, a thiol-dependent reductase. Identification of its secretory form and inducible expression by the oncogenic transformation. *Eur. J. Biochem.* 234:336–342.

Holmgren, A. 1979. Thioredoxin catalyzes the reduction of insulin disulfides by dithiothreitol and dihydrolipoamide. *J. Biol. Chem.* 254:9627–9632.

Hughes, E.A., and P. Cresswell. 1998. The thiol oxidoreductase ERp57 is a component of the MHC class I peptide-loading complex. *Curr. Biol.* 8:709–712.

Hwang, C., A.J. Sinskey, and H.F. Lodish. 1992. Oxidized redox state of glutathione in the endoplasmic reticulum. *Science.* 257:1496–1502.

John, L.M., J.D. Lechleiter, and P. Camacho. 1998. Differential modulation of SERCA2 isoforms by calreticulin. *J. Cell Biol.* 142:963–973.

Kaufman, R.J. 1999. Stress signaling from the lumen of the endoplasmic reticulum: coordination of gene transcriptional and translational controls. *Genes Dev.* 13:1211–1233.

Kostova, Z., and D.H. Wolf. 2003. For whom the bell tolls: protein quality control of the endoplasmic reticulum and the ubiquitin-proteasome connection. *EMBO J.* 22:2309–2317.

Leach, M.R., M.F. Cohen-Doyle, D.Y. Thomas, and D.B. Williams. 2002. Localization of the lectin, ERp57 binding, and polypeptide binding sites of cal-

nexin and calreticulin. *J. Biol. Chem.* 277:29686–29697.

Li W., J. Llopis, M. Whitney, G. Zlokarnik, and R.Y. Tsien. 1998. Cell-permeant caged InsP3 ester shows that Ca21 spike frequency can optimize gene expression. *Nature*. 392:936–941.

Lindquist, J.A., O.N. Jensen, M. Mann, and G.J. Hammerling. 1998. ER-60, a chaperone with thiol-dependent reductase activity involved in MHC class I assembly. *EMBO J.* 17:2186–2195.

Marcus, N., D. Shaffer, P. Farrar, and M. Green. 1996. Tissue distribution of three members of the murine protein disulfide isomerase (PDI) family. *Biochim. Biophys. Acta.* 1309:253–260.

Mogami, H., A.V. Tepikin, and O.H. Petersen. 1998. Termination of cytosolic Ca^{2+} signals: Ca^{2+} reuptake into intracellular stores is regulated by the free Ca^{2+} concentration in the store lumen. *EMBO J.* 17:435–442.

Morrice, N.A., and S.J. Powis. 1998. A role for the thiol-dependent reductase ERp57 in the assembly of MHC class I molecules. *Curr. Biol.* 8:713–716.

Oliver, J.D., F.J. van der Wal, N.J. Bulleid, and S. High. 1997. Interaction of the thiol-dependent reductase ERp57 with nascent glycoproteins. *Science.* 275: 86–88.

Oliver, J.D., H.L. Roderick, D.H. Llewellyn, and S. High. 1999. ERp57 functions as a subunit of specific complexes formed with the ER lectins calreticulin and calnexin. *Mol. Biol. Cell.* 10:2573–2582.

Patil, C., and P. Walter. 2001. Intracellular signaling from the endoplasmic reticulum to the nucleus: the unfolded protein response in yeast and mammals. *Curr. Opin. Cell Biol.* 13:349–355.

Pozzan, T., R. Rizzuto, P. Volpe, and J. Meldolesi. 1994. Molecular and cellular physiology of intracellular calcium stores. *Physiol. Rev.* 74:595–636.

Ramsden, M., M. Murray, Z. Henderson, H.A. Pearson, V.A. Campbell, and J. Jeffery. 2000. Apoaequorin monitors degradation of endoplasmic reticulum (ER) proteins initiated by loss of ER Ca^{2+}. *J. Biol. Chem.* 275:4713–4718.

Roderick, H.L., J.D. Lechleiter, and P. Camacho. 2000. Cytosolic phosphorylation of calnexin controls intracellular Ca^{2+} oscillations via an interaction with SERCA2b. *J. Cell Biol.* 149:1235–1248.

Ruiz-Perez, V.L., S.A. Carter, E. Healy, C. Todd, J.L. Rees, P.M. Steijlen, A.J. Carmichael, H.M. Lewis, D. Hohl, P. Itin, et al. 1999. ATP2A2 mutations in Darier's disease: variant cutaneous phenotypes are associated with missense mutations, but neuropsychiatric features are independent of mutation class. *Hum. Mol. Genet.* 8:1621–1630.

Sakuntabhai, A., V. Ruiz-Perez, S. Carter, N. Jacobsen, S. Burge, S. Monk, M. Smith, C.S. Munro, M. O'Donovan, N. Craddock, et al. 1999. Mutations in ATP2A2, encoding a Ca^{2+} pump, cause Darier disease. *Nat. Genet.* 21: 271–277.

Schrag, J.D., J.J. Bergeron, Y. Li, S. Borisova, M. Hahn, D.Y. Thomas, and M. Cygler. 2001. The structure of calnexin, an ER chaperone involved in quality control of protein folding. *Mol. Cell.* 8:633–644.

Schrag, J.D., D.O. Procopio, M. Cygler, D.Y. Thomas, and J.J. Bergeron. 2003. Lectin control of protein folding and sorting in the secretory pathway. *Trends Biochem. Sci.* 28:49–57.

Stevens, F.J., and Y. Argon. 1999. Protein folding in the ER. *Semin. Cell Dev. Biol.* 10:443–454.

Sun, J., L. Xu, J.P. Eu, J.S. Stamler, and G. Meissner. 2001. Classes of thiols that influence the activity of the skeletal muscle calcium release channel. *J. Biol. Chem.* 276:15625–15630.

Van der Wal, F.J., J.D. Oliver, and S. High. 1998. The transient association of ERp57 with N-glycosylated proteins is regulated by glucose trimming. *Eur. J. Biochem.* 256:51–59.

Vassilakos, A., M. Michalak, M.A. Lehrman, and D.B. Williams. 1998. Oligosaccharide binding characteristics of the molecular chaperones calnexin and calreticulin. *Biochemistry.* 37:3480–3490.

Welihinda, A.A., W. Tirasophon, and R.J. Kaufman. 1999. The cellular response to protein misfolding in the endoplasmic reticulum. *Gene Expr.* 7:293–300.

Xia, R., T. Stangler, and J.J. Abramson. 2000. Skeletal muscle ryanodine receptor is a redox sensor with a well defined redox potential that is sensitive to channel modulators. *J. Biol. Chem.* 275:36556–36561.

Zable, A.C., T.G. Favero, and J.J. Abramson. 1997. Glutathione modulates ryanodine receptor from skeletal muscle sarcoplasmic reticulum. Evidence for redox regulation of the Ca^{2+} release mechanism. *J. Biol. Chem.* 272:7069–7077.

Zapun, A., N.J. Darby, D.C. Tessier, M. Michalak, J.J. Bergeron, and D.Y. Thomas. 1998. Enhanced catalysis of ribonuclease B folding by the interaction of calnexin or calreticulin with ERp57. *J. Biol. Chem.* 273:6009–6012.